VSP

Journal of Biomaterials Science 21 (2010) 1297–1312

Journal of BIOMATERIALS SCIENCE
brill.nl/jbs

Characterization of Poly(ε-caprolactone)/Polyfumarate Blends as Scaffolds for Bone Tissue Engineering

Juan Manuel Fernandez [a,b], **M. Silvina Molinuevo** [b], **Ana M. Cortizo** [b], **Antonio D. McCarthy** [b] **and M. Susana Cortizo** [a,*]

[a] Instituto de Investigaciones Fisicoquímica Teóricas y Aplicadas (INIFTA), Facultad de Ciencias Exactas, Universidad Nacional de La Plata, CC 16 Suc. 4, 1900 La Plata, Argentina
[b] GIOMM (Grupo de Investigación en Osteopatías y Metabolismo Mineral), Departamento de Ciencias Biológicas, Facultad de Ciencias Exactas, Universidad Nacional de La Plata, 1900 La Plata, Argentina

Received 27 May 2009; accepted 28 July 2009

Abstract

There is considerable interest in the design of polymeric biomaterials that can be used for the repair of bone defects. In this study, we used ultrasound to prepare a compatibilized blend of poly(ε-caprolactone) (PCL) and poly(diisopropyl fumarate) (PDIPF). The formation of post-sonication inter-polymer coupling products was verified by SEC analysis of a blend with azo-labeled PDIPF. We also analyzed the physicochemical and mechanical properties of the compatibilized blend. When compared to PCL alone, the PCL/PDIPF blend showed no difference in its resistance as evaluated by the elastic modulus, although it did show a 50% decrease in ultimate tensile stress ($P < 0.05$) and an 84% decrease in elongation-at-break ($P < 0.05$). However, the mechanical properties of this blend were comparable to those of trabecular bone. We next evaluated biocompatibility of the PCL/PDIPF blend, and of homo-polymeric PCL and PDIPF films for comparison, with UMR106 and MC3T3E1 osteoblastic cells. Osteoblasts plated on the compatibilized blend adhered and proliferated more than on either homo-polymer, showed a greater number of cellular processes with a better organized actin cytoskeleton and expressed more type-I collagen and mineral, both markers of osteoblast phenotype. These results support the hypothesis that this new compatibilized blend could be useful in future applications for bone regeneration.

Keywords

Bone tissue engineering, biocompatibility, poly(ε-caprolactone), poly(dialkyl fumarates), ultrasound

* To whom correspondence should be addressed. Tel.: (54-221) 425-7430; Fax: (54-221) 425-4642; e-mail: gcortizo@inifta.unlp.edu.ar

 DOI:10.1163/092050609X12517190417632

1. Introduction

In the past years, there has been considerable interest in the area of bone tissue engineering, particularly for the design of biomaterials which can substitute and repair damaged bone. Different synthetic or natural polymers, as well as composites, have been used as scaffolds for bone defect sites [1–3]. To be useful, these biomaterials need to possess a number of specific properties that include: lack of immunogenicity, a timely biodegradation rate which allows for adequate growth of the new tissue, non-toxic degradation products, and appropriate mechanical properties in order to provide structural stability to a bone defect site while resilient to mechanical stress [4].

Osteoinduction and osteoconduction are essential elements for bone regeneration, along with osteointegration which is the final bonding between host bone and the polymeric grafting material [5]. Osteoinduction is the stimulation and differentiation of host mesenchymal cells from the surrounding tissue into bone-forming osteoblasts, and can be enhanced if osteogenic factors are included in the polymeric graft material (i.e., the scaffold as an osteogenic delivery system). Osteoconduction, on the other hand, relates to the ability of the polymer to facilitate and orient new blood vessels and Haversian systems into the scaffold, and is related to its porosity. A porous surface also favours osteointegration, since it improves mechanical interlocking between the implant biomaterial and the surrounding natural bone [6].

Although various polymeric materials have been investigated for bone tissue engineering, no single polymer has been found to meet all the requirements needed for a bone scaffold. Each polymer possesses its characteristic advantages and disadvantages. On the other hand, composite materials often show an adequate balance of desirable properties, and frequently also improved characteristics compared to their individual components (natural bone matrix is no exception, since it is an organic/inorganic composite material). From this standpoint, in theory composite materials are probably superior as bone tissue engineering scaffolds [7].

Poly(ε-caprolactone) (PCL) is a biocompatible, biodegradable and semi-crystalline polyester that has previously been proposed for biomedical applications [8]. Its slow rate of hydrolytic degradation makes this polymer useful for long-term applications [9]. Its porosity and crystallinity and, thus, the mechanical properties of the polymer are dependent on the PCL concentration in the cast film. In order to improve these properties for its possible use in bone lesions, blending with other materials has been approached [10]. On the other hand, homo-polyalkyl fumarates have a skeleton composed of a linear structure of C–C, which reduces their biodegradability in comparison with polyesters. In addition, polyfumarates can be expected to exhibit better mechanical properties than polyesters.

In recently published work we began to evaluate the possible use as bone scaffolds, of polyesters (PCL) and polyfumarates prepared by casting. In those experiments we found that they were able to support osteoblastic growth, and in addition were biodegradable by hydrolytic and cellular mechanisms [11]. The PCL film showed a rougher and more porous surface than the polyfumarate film. In addition,

osteoblastic proliferation was comparable to control conditions, demonstrating the biocompatibility of both surfaces. Based on these previous results, we hypothesized that blending both polymers could be of interest for bone tissue engineering, if it were to generate a material that combined the best properties of each individual polymer (e.g., adequate porosity, elastic and tensile properties and biocompatibility).

In the present study we have prepared a biomimetic bone scaffold based on PCL and poly(diisopropyl fumarate) (PDIPF) blends obtained by sonication. In addition, we have analyzed the physicochemical, mechanical and biological properties of these blends to evaluate their possible use as scaffolds for the repair of bone defects.

2. Materials and Methods

2.1. Synthesis and Characterization of Polymers

Poly(diisopropyl fumarate) (PDIPF) was synthesized by microwave-assisted radical polymerization using benzoyl peroxide as initiator [12]. Briefly, 1 g monomer was added to a previously weighed amount of initiator (30 mM) under nitrogen gas into a 25 cm^3 conical Pyrex flask closed by a septum. The reactor was submitted to different times and power of irradiation using a domestic microwave oven (Zenith, ZVP-2819). After reaction, the polymers were isolated and purified by solubilization–precipitation (toluene/methanol = 1:8) and dried until constant weight was achieved. In this study a sample of weight-average molecular weight (M_w) and polydispersity index (PDI) of 131 kg/mol and 2.0, respectively, was used.

PCL was purchased from Aldrich and has a M_w and PDI of 65 kg/mol and 1.4, respectively, as indicated by the manufacturer.

The M_w and molecular weight distribution were determined by size-exclusion chromatography (SEC) in a LKB-2249 instrument at 25°C. A series of μ-Styragel columns, with pore sizes 10^5, 10^4, 500, 100 Å, were used with chloroform as an eluent. The polymer concentration was 4–5 mg/ml and the flow rate was 0.5 ml/min. The polymer was detected at 5.75 μm with a Miran 1A infrared spectrophotometer detector and calibration was performed using poly(methyl methacrylate) as a standard.

2.2. Polymer Blends

Compatibilized blends of PCL and PDIPF were obtained by ultrasound using a Bandelin HD60 at 20°C. In order to determine the optimal conditions of blend compatibilization, a preliminary assay was carried out using PDIPF with the fluorescent end-group 3-phenylazobenzoyle [13]. This polymer, designated as PDIPF*, has a M_w and PDI of 83 kg/mol and 2.1, respectively, as determined by SEC. Briefly, a 1 wt% solution of a PCL/PDIPF blend (75:25 (w/w)) or homo-polymer was prepared in chloroform and dissolution was facilitated by stirring into a shaker overnight at room temperature. The solution was sonicated (37 W) at 20°C, 1-ml

aliquots were removed from the reaction mixture at different times, filtrated through a 0.45-μm Teflon membrane and the M_w was analyzed by SEC.

A physical blend of PCL and PDIPF was obtained by mixture of the two homopolymers in chloroform (75:25 (w/w)), for comparison.

2.3. Preparation of the Films

In order to perform experiments with osteoblastic cells in culture, scaffolds of homo-polymers or blends were cast as films. This kind of samples allows us to evaluate with a light microscope the morphology and the growth of these cells. Polymer films were prepared by solvent casting methodologies: a solution was prepared of the polymer blend (physical or compatibilized) — or of polymer alone — in chloroform (5% (w/w)) and was poured onto glass Petri dishes (19.6 cm^2). The solvent was allowed to evaporate at room temperature, and then the resulting films were dried under vacuum until constant weight. The films were sterilized by UV exposition for 2 h. SEC confirmed that no degradation of the material had occurred during this treatment.

2.4. Scanning Electron Microscopy

The surfaces of the matrices were coated with gold and their morphology was examined using scanning electron microscopy (SEM, Philips 505), with an accelerating voltage of 20 kV. The images were analyzed by Soft Imaging System ADDAII. Alternatively scaffolds were seeded with osteoblastic cells for 24 h. Scaffolds were fixed with 96% ethanol for 10 min at room temperature. After that, samples were dehydrated with graded ethanol series and finally dried at room temperature and coated with gold. The samples were analyzed as above.

2.5. Mechanical Testing

Mechanical properties of polymeric scaffolds were determined with a universal testing machine (Digimess TC500) using force load cell of 50 N capacity at room temperature, in tensile mode [14]. The dog-bone-shaped specimens (50×18 mm^2) were tested at a rate of 5 mm/min until breaking point. Ultimate tensile stress, elastic modulus, as well as elongation-at-break were calculated on the basis of the generated tensile stress–strain curves. The results presented are the mean values of eight independent measurements.

2.6. Cell Culture and Incubation

UMR106 rat osteosarcoma cells and MC3T3E1 mouse calvaria-derived cells were grown in DMEM containing 10% FBS, 100 U/ml penicillin and 100 μg/ml streptomycin at 37°C in a 5% CO_2 atmosphere [15]. Cells were seeded on 75 cm^2 flasks and sub-cultured using trypsin-EDTA. The UMR106 cell line has been shown to conserve certain characteristics of differentiated osteoblastic phenotype [16]. For the different experiments, cells were seeded on polymeric matrix-coated dishes and were incubated in 10% FBS–DMEM during the periods of time indicated in the

figure legends. For ALP expression and type-I collagen production and mineralization experiments with MC3T3E1 osteoblasts, cells were cultured for 2 or 3 weeks in DMEM/FBS supplemented with β-glycerol-phosphate and ascorbic acid (osteogenic media), changing the medium every 2 days.

2.7. Cell Adhesion and Proliferation

The adhesion assay was performed as reported previously [11, 17]. Briefly, cells were plated in DMEM-10% FBS on a polymeric matrix at a seeding density of 10^5 cells/ml, and allowed to adhere for 1 h at 37°C. For proliferation studies, cells were cultured for 24 h. At the end of the incubation period, osteoblasts were washed with PBS, fixed with methanol and stained with Giemsa as we have previously described [11]. The number of cells on each scaffold was evaluated by microscopy, counting several representative fields per well.

2.8. Cell Morphology

An immunofluorescent assay for actin fibers was used to analyze possible changes in cell cytoskeleton morphology, as well as in osteoblast integration/interactions with biomaterials. Osteoblasts were cultured in DMEM-10% FBS on polymeric matrix for 24 h. After this incubation period, cells were fixed with 4% *p*-formaldehyde in PBS for 15 min, permeabilized with cold methanol for 4 min, and stained with fluorescein-labelled phalloidin (1:100) in the dark for 1 h at room temperature. Samples were mounted in Vectashield Mounting Medium with DAPI (stain for nuclei). Images were recorded and analysed using a BX51 model-Olympus fluorescence microscope and a DP Controller image processor.

2.9. Evaluation of Markers for Osteoblastic Phenotype

The ability of the cells to express markers of osteoblastic phenotype associated with bone-forming capacity was evaluated by measurement of alkaline phosphatase (ALP) activity and collagen production [18]. Briefly, for ALP determination, cells were washed with PBS and solubilized in 0.5 ml 0.1% Triton X-100. Aliquots of this total cell extract were used for protein determination by the Bradford technique [19], and for measurement of ALP by spectrophotometric determination of initial rates of hydrolysis of *para*-nitrophenyl-phosphate (p-NPP) to *para*-nitrophenol (p-NP) at 37°C for 10 min. The production of p-NP was determined by absorbance at 405 nm. Under our experimental conditions p-NP production was linear for 15 min. For type-I collagen production, cells were fixed in Bouin's fluid for 1 h, washed with water and stained with Sirius-Red S dye for 1 h [11]. After that, the stained material was dissolved in 0.1 M NaOH and the absorbance read at 550 nm. Mineralized nodules in the extracellular matrix of MC3T3E1 osteoblasts were stained with Alizarin-Red S [18].

2.10. Statistical Analysis

Results are expressed as mean $\pm$ SEM and, unless indicated otherwise, were obtained from two separate experiments performed in triplicate. Differences between

the groups were assessed by one-way ANOVA with Tukey post-hoc test. For non-normal distributed data, a non-parametrical Kruskal–Wallis with Dunn post-hoc test was performed using GraphPad In Stat version 3.00 (Graph Pad Software). A P value < 0.05 was considered significant for all statistical analyses.

3. Results and Discussion

3.1. Characterization of Polymer Blends

Polymer blending is an effective way to achieve a desirable combination of properties that are often absent in single homo-polymers. However, in most cases the simple blending of two polymers does not produce good results, due to the incompatibility of the blend. Some studies have demonstrated that due to chain scission with macroradical formation, sonochemically induced reactions can lead to inter-polymer radical coupling and measurable block co-polymer which is useful for reactive compatibilization [20, 21]. We have used this methodology in order to obtain PCL/PDIPF compatible blends. Figure 1a shows the relative change of

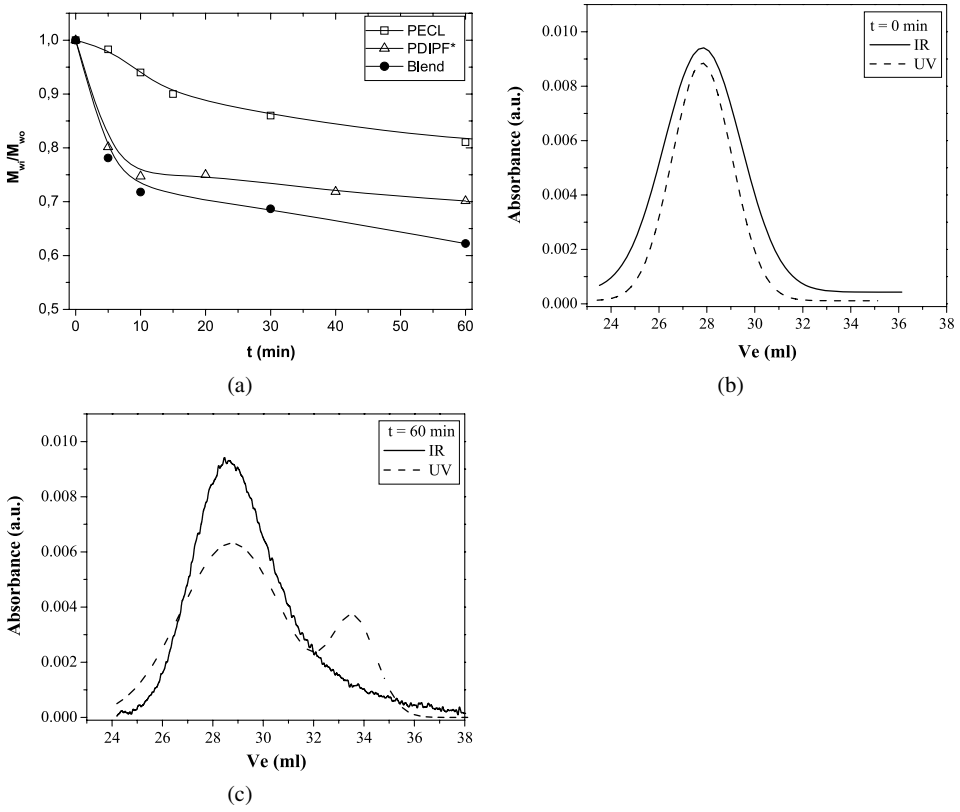

Figure 1. (a) Evolution of relative changes in weight-average molecular weight of the three samples studied as a function of sonication time. Chromatogram of labeled PDIPF/PCL blend at (b) 0 and (c) and 60 min sonication.

weight-average molecular weight, $M_{w,i}/M_{w,o}$, as a function of the sonication time. $M_{w,i}$ and $M_{w,o}$ are the weight-average molecular weights of the polymer at a fixed time and at the initial time. From Fig. 1a it can be seen that the blend and PDIPF* were degraded faster than PCL, and that in all cases a decrease of the degradation rate was observed after 10 min. This result is in agreement with other sonication studies, which have reported that chain scission attains a limiting molecular weight below which no further degradation occurs [22, 23]. The formation of post-sonication inter-polymer coupling products was verified by SEC of a blend that included an azo-labeled PDIPF (Fig. 1b and 1c). This polymer, obtained by radical polymerization with 3-phenylazobenzoyl peroxide, was spectroscopically detected at 320 nm by a UV-visible detector. The carbonyl group present in the chain of PCL and PDIPF allows the detection of both polymers at 5.75 μm using an Infrared detector. The chromatogram centred at 27.8 ml, shown in Fig. 1b, represents the blend of PCL and PDIPF* polymers at initial time. Figure 1c shows the corresponding chromatogram after 60 min sonication. After exposing the solution blend to high-intensity ultrasound the SEC chromatogram exhibited a bimodal molecular weight distribution: the first peak appeared at 28.8 ml elution volume, while the second peak, at a later elution volume (33.5 ml), corresponded to a lower molecular weight. This second peak can be attributed to inter-polymer radical reaction products. Although the block co-polymer was not isolated, the UV-detection put in evidence its presence. These experiments demonstrate that a PCL/PDIPF blend may be compatibilized through a block co-polymer created during sonication. Lebovitz *et al*. have also demonstrated the presence of a block co-polymer using a similar procedure [20]. This methodology seems to be a simple, accessible and a low time-consuming procedure.

Figure 2 shows the SEM images of films obtained from the compatibilized blend (Fig. 2a), a physical blend (Fig. 2b) and the two homo-polymers for comparison (Fig. 2c and 2d). The compatibilized PCL/PDIPF blend (Fig. 2a) shows a more homogeneous surface than the physical blend. Figure 2b shows that the physical blend exhibited great phase separation, with an irregular and rough surface corresponding to the PDIPF phase dispersed in the continuous PCL phase. In addition, the compatibilized PCL/PDIPF blend (Fig. 2a), the physical mixture (Fig. 2b) and PCL (Fig. 2c) show the typical spherulite-like morphology previously described for PCL by other authors [24]. However, the physical blend shows a coarser phase size than that of the compatibilized blend. Finally, PDIPF presents a smooth surface (Fig. 2d). In all, these results suggest that the ultrasound compatibilized blend presents adequate homo-polymeric integration.

Important requirements for scaffold materials are their mechanical properties, which must be adequate so that they do not collapse during handling and during the patient's normal activities [25]. Bones belonging to the axial skeleton are predominantly submitted *in vivo* to compressive forces, while bones from the appendicular skeleton must support principally tensile forces. In this context, materials designed for use as scaffolds for bone repair may be evaluated by their tensile and/or com-

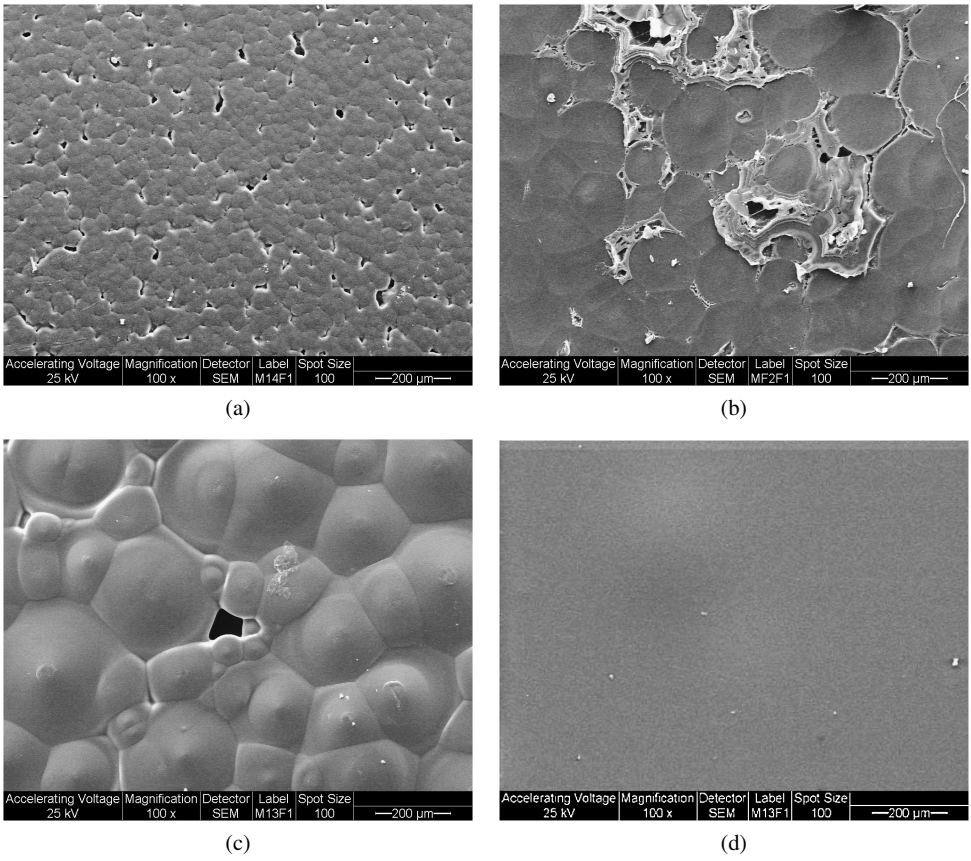

Figure 2. Scanning electron microscopy of the (a) compatibilized blend, (b) physical blend, (c) PCL film and (d) PDIPF film.

pressive mechanical properties (as well as their elastic modulus), depending on their intended use.

PDIPF is known to be a brittle material with a high tensile strength, but these properties can be changed by blending with other polymers [26], such as we have performed in the present study. Table 1 shows the mechanical properties evaluated for the compatibilized blend, the physical blend and PCL on its own for comparison. It is possible to see that the addition of PDIPF to PCL does not significantly affect the resistance of the scaffold as evaluated by the elastic modulus. However, the blends (compatibilized or physical) induce changes in other mechanical properties. Such changes are reflected by a nearly 50% decrease in ultimate tensile stress ($P < 0.05$), and 84% and 62% decrease in elongation-at-break of compatibilized and physical blends, respectively ($P < 0.05$). The elongation-at-break point, a measurement of the ductility of a material, showed a statistically significant decrease in both blends, due to the effect of the stiffer PDIPF. Other authors have evaluated the mechanical properties of cortical and trabecular bone [27, 28]. In particular, tra-

Table 1.
Mechanical properties of compatibilized PCL/PDIPF blends, physical PCL/PDIPF blends and PCL homo-polymeric films

Sample	Elastic modulus (MPa)	Ultimate tensile stress (MPa)	Elongation-at-break (%)
Compatibilized blend	143 ± 12	7.5 ± 0.7	60 ± 12
Physical blend	110 ± 26	6.4 ± 1.7	75 ± 4
PCL	161 ± 12	$15.2 \pm 1.7^*$	$366 \pm 96^*$

Results are expressed as the mean $\pm$ SEM, $n = 8$. $^*P < 0.05$.

becular/cancellous bone possesses an ultimate tensile stress which is very similar to that of our PCL/PDIPF blends, although with an elastic modulus three times greater, indicating that trabecular bone is somewhat stiffer than our polymeric blend. This slight difference in mechanical properties could nevertheless be overcome by the incorporation of an inorganic and osteoinductive additive to the polymer, such as hydroxyapatite. Experiments are under way in our laboratory to address this issue, and will be presented as part of a different manuscript.

3.2. Biocompatibility Studies

The biocompatibility of the compatibilized PCL/PDIPF blend was evaluated by its capacity to support the adhesion, proliferation and differentiation of osteoblastic cells. We also studied possible changes in osteoblastic morphology and cytoskeleton. PCL and PDIPF films were used for comparison. The UMR106 cells plated on polymer scaffolds were fixed, stained with Giemsa and observed by light microscopy in order to assess adhesion of osteoblasts after 1 h incubation. As we have described previously, cell monolayers growing on standard tissue culture polystyrene dishes exhibit a polygonal morphology with cytoplasmic processes [29]. In the present work, although the polymer blends as well as the PCL films are slightly opaque (Fig. 3a and 3b), cells adhering onto those polymeric matrices displayed a circular morphology with extension of filopodia. Cells plated on these matrices also seemed to be more deeply included inside the films. On the other hand, osteoblasts attached to the PDIPF matrix were more picnotic and rounded in shape and appeared in isolation or forming cell clumps on the surface. The fact that the cells were seen included inside the blend and PCL matrices could be advantageous for osteoblastic differentiation. The quantification of osteoblastic adhesion to homo-polymer or polymer blend films is shown in Fig. 3b. The number of osteoblasts that adhere to the polymer blend film was significantly higher than the cells attached to the PDIPF or PCL homo-polymeric films ($P < 0.05$).

The possible interaction of osteoblasts with different polymeric films was also investigated by evaluating changes in actin cytoskeleton, after 24 h of culture. Representative immunofluorescent microscopic images of cells observed using $1000\times$ total magnification are presented in Fig. 4. Osteoblasts, growing on polymer blend

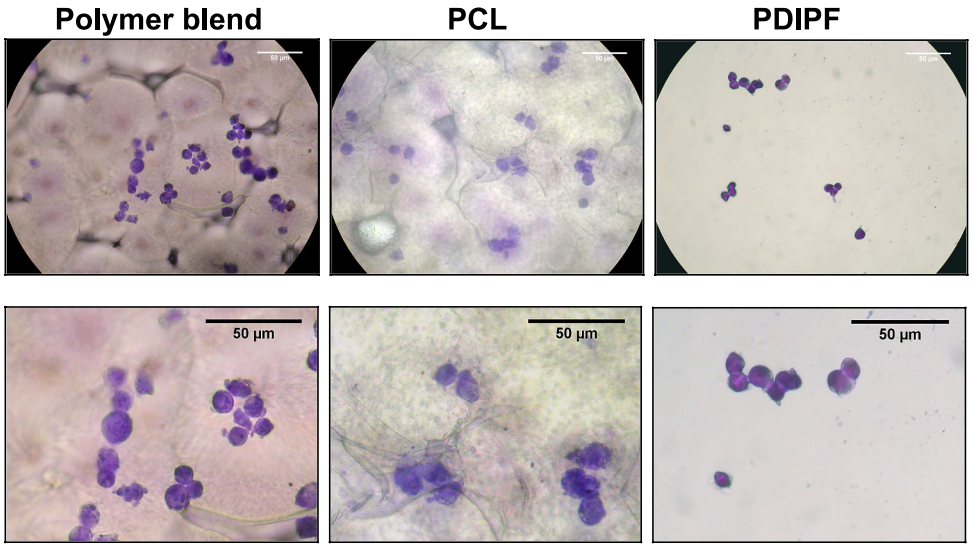

(a)

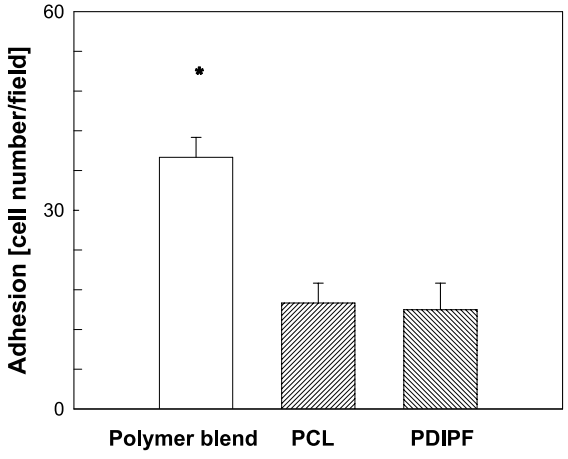

(b)

Figure 3. Effect of blending on the adhesion of UMR106 osteoblasts. Cells were plated and incubated on different films. (a) Light micrographs of cells stained with Giemsa. Higher magnification shows a rounded morphology. (b) Quantitation of adhesion was assessed by counting the number of cells per field in 10 representative fields per film. Values are shown as the mean ± SEM. $^{*}P < 0.05$. This figure is published in colour in the online edition that can be accessed *via* http://www.brill.nl/jbs

films and individually identified by DAPI staining of nuclei (blue), exhibited a well-developed actin cytoskeleton with clearly observed stress fibers. Cells growing on PDIPF and PCL films displayed a different morphology with a disorganized peripheral actin ring and a rounded shape.

These results are to be expected if the balance between hydrophobicity and hydrophilicity of the different polymers is taken into account. PDIPF is more hy-

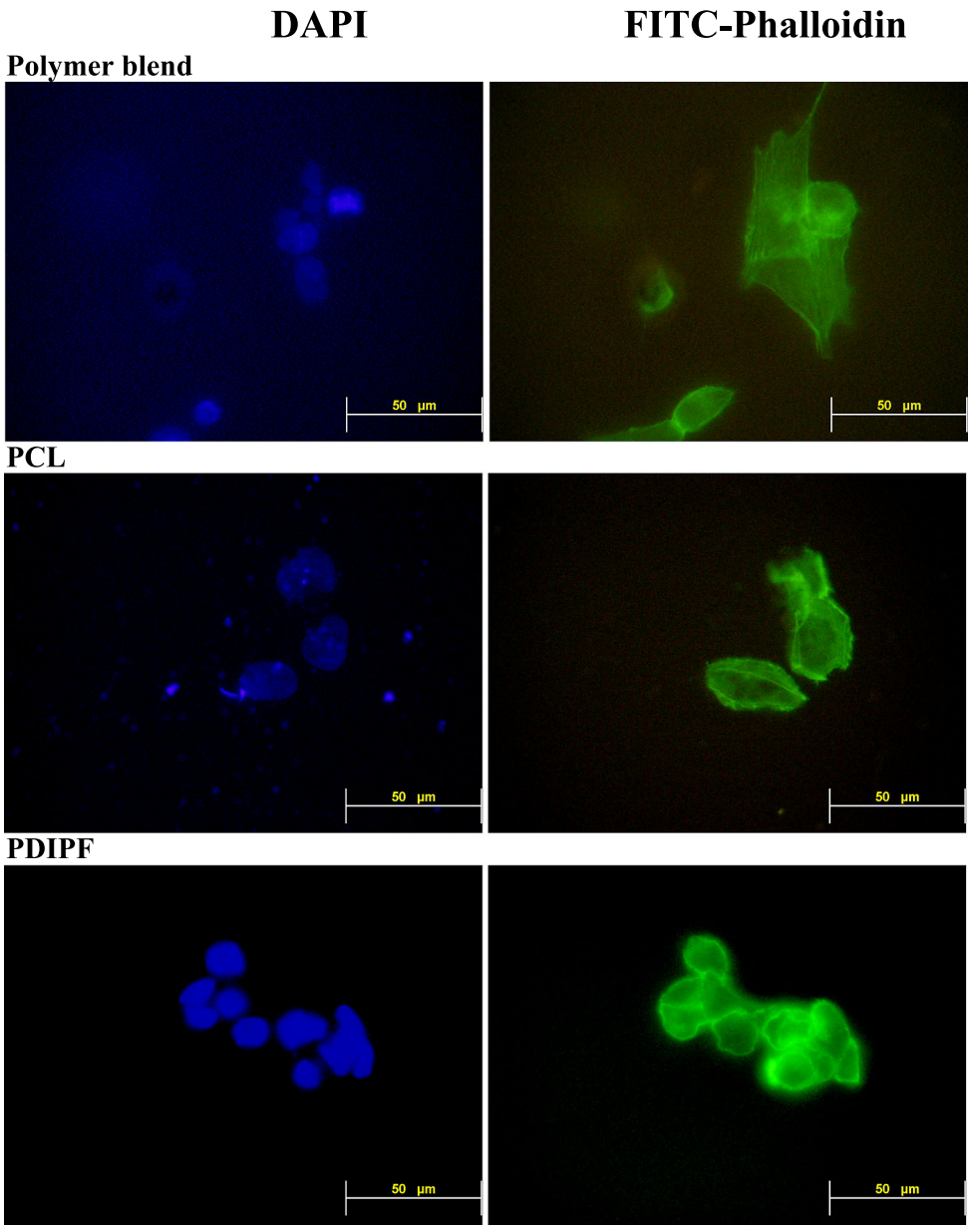

Figure 4. Cytoskeleton organization and nuclei morphology of UMR106 cells cultured on different films. Cells were cultured for 24 h on PDIPF/PCL blend, PCL or PDIPF polymeric matrixes. Fixed cells were stained for actin (green) with FITC-phalloidin and for nuclei (blue) with DAPI, and analyzed by fluorescence microscopy. This figure is published in colour in the online edition that can be accessed *via* http://www.brill.nl/jbs

drophobic and, thus, induces cell clumping (Figs 3 and 4). PCL is more hydrophilic, whereas the compatibilized blend possesses an adequate balance between both

properties that supports efficient cell adhesion with abundant cellular extensions or philopodia (Fig. 3) and the formation of a more organized actin cytoskeleton (Fig. 4). We have previously shown that UMR106 osteoblastic cells can attach to a type-I collagen substratum *via* $\alpha 1, 5\beta 1$ and $\alpha 2\beta 1$ integrin receptors [17]. However, when the cells are seeded on a surface that is not coated by extracellular matrix proteins (ECM), such as the polymers evaluated in the present study, cellular attachment depends on their timely secretion of ECM [30]. This secretion could be increased in our experiments with the compatibilized PCL/PDFIP blends, and probably accounts for the observed increase in osteoblastic attachment and actin cytoskeleton organization.

Cells seeded on polymer scaffolds were further cultured for 24 h and evaluated either by Giemsa staining and light microscopy to assess cell proliferation, or by SEM to determine formation of cell extensions. Figure 5a and 5b shows that osteoblastic cells grow about 60% less on the PCL film and 85% less on the PDIPF film, when compared with the polymeric blend. In addition, cells grown on the compatibilized polymer blend showed a greater number of philopodia than on homo-polymeric scaffolds (Fig. 5c). These observations suggest that osteoblastic cells grow better on the polymer blend than on the homo-polymer films.

We also evaluated the capacity of cells growing on different matrices to express two markers of bone forming cells. Figure 6a and 6b shows the expression of ALP after culturing osteoblasts by 48 h. This parameter was not affected by the nature of the matrix investigated. Type-I collagen production, the main extracellular matrix protein expressed in bone, was also evaluated. As can be seen in Fig. 6c, more collagen was produced by the UMR106 cells growing on the polymer blend, suggesting a better affinity with this material. However, when MC3T3E1 line was cultured for 2 weeks in an osteogenic medium, cells produced more collagen in the PCL matrix (Fig. 6d). These observations suggest that some degree of specificity on osteblastic development does depend on the cell line used in the studies. Furthermore, the effect of the different polymeric scaffolds on the ability of MC3T3E1 cells to mineralize the matrix was assessed after 3 weeks of culture in the presence of β-glycerol phosphate and ascorbic acid. Figure 6e shows that the blend strongly promotes the deposition in mineralized nodules as assessed by the Alizarin-Red S staining, in comparison with the homo-polymer films.

4. Conclusions

We have prepared a new PDIPF/PCL blend obtained by ultrasonic compatibilization through the block co-polymer created during sonication. This blend exhibited better surface characteristics than that of the physical mixtures. The analysis of its mechanical properties suggests a similarity with trabecular bone and a possible application in bone tissue engineering.

Biocompatibility studies did not show evidence of cytotoxic effects when cells were cultured on the PDIPF/PCL blend. On the contrary, cells were able to grow,

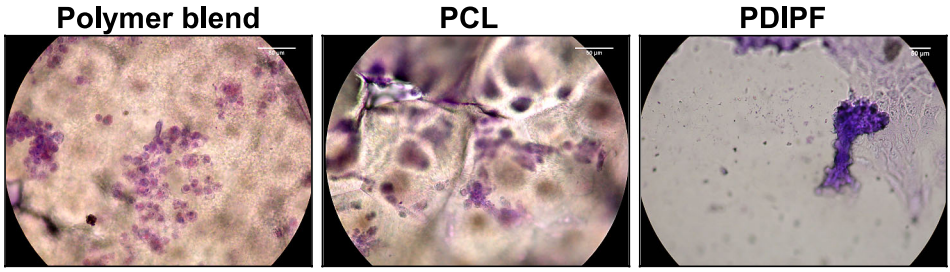

(a)

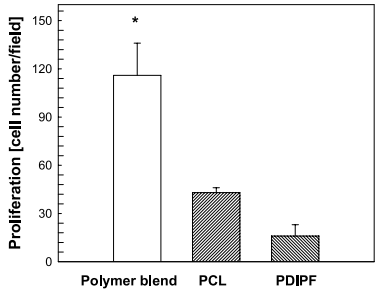

(b)

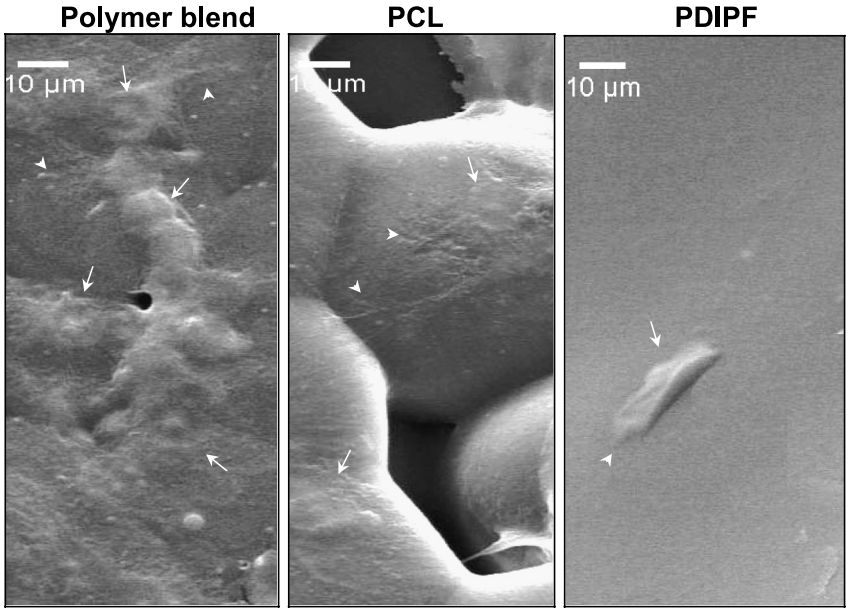

(c)

Figure 5. Effect of blending on the proliferation and morphology of UMR106 osteoblasts. Cells were plated and cultured on different films for 24 h. (a) Light micrographs of cells stained with Giemsa. (b) Quantitation of proliferation was assessed by counting the number of cells per field in 10 representative fields per film. Values are shown as the mean ± SEM. $^{*}P < 0.05$. (c) Scanning electron microscopy of cells growing on different films. Arrows indicate cells and head of arrows show the cell extensions. This figure is published in colour in the online edition that can be accessed *via* http://www.brill.nl/jbs

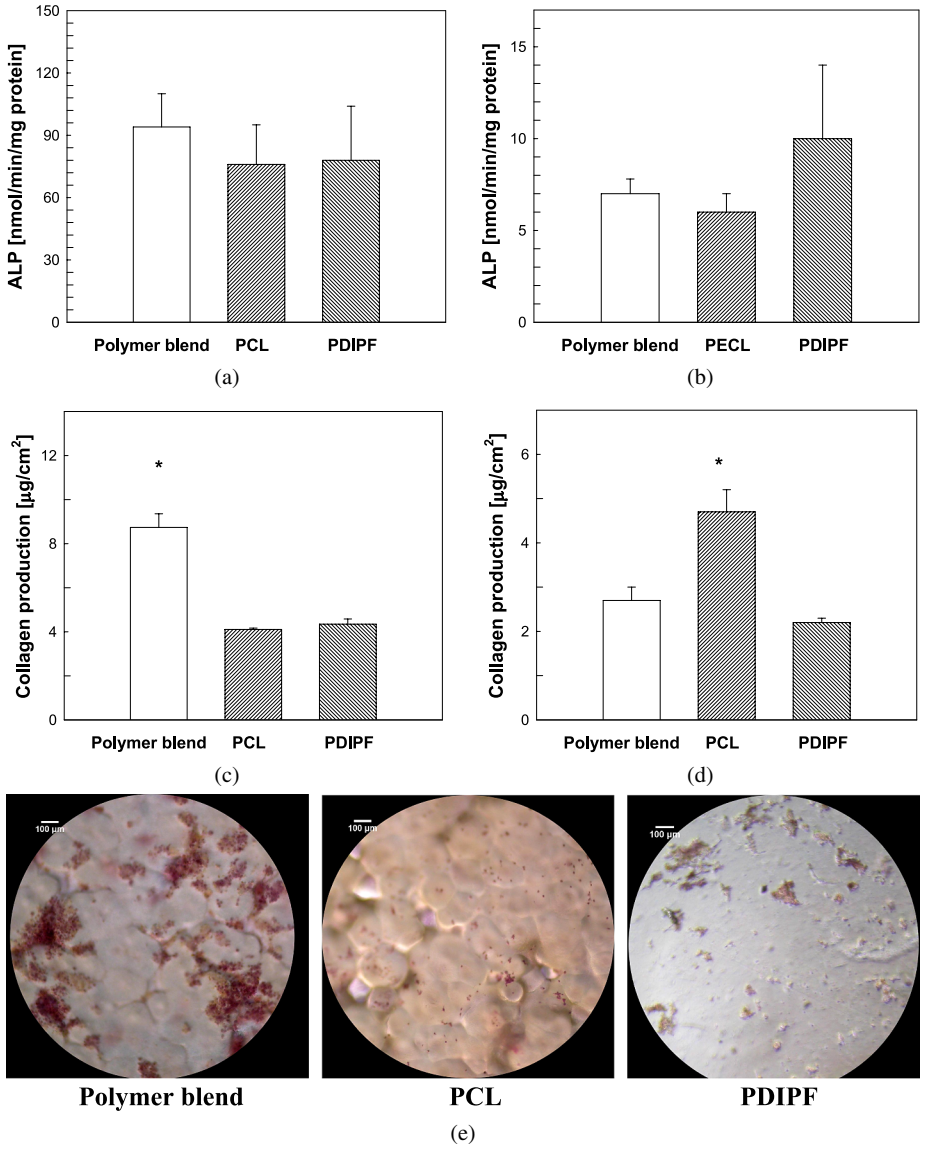

Figure 6. Effect of the matrix on the expression of osteoblastic markers and mineralization. UMR106 (a, c) or MC3T3E1 (b, d) were cultured on different films for 48 h or 2 weeks, respectively. ALP (a, b) and type-I collagen production (c, d) were evaluated as described in Materials and Methods. Values represent the mean ± SEM. $^{*}P < 0.05$. (e) MC3T3E1 cells were cultured for 3 weeks on different polymeric films in the presence of an osteogenic media. Mineralized nodules were assessed by Alizarin-Red S staining. This figure is published in colour in the online edition that can be accessed *via* http://www.brill.nl/jbs

to develop extensions that interacted with the blend surface and to express different markers of osteoblastic phenotype on this new material. Moreover, MC3T3E1 cells

were able to deposit more mineral in the blend scaffold. All together, these results support the hypothesis that this new compatibilized blend could be useful in future applications for bone regeneration.

Acknowledgements

This work was partially supported by grants from Universidad Nacional de La Plata (UNLP), Facultad de Ciencias Exactas, Comisión de Investigaciones Científicas de la Provincia de Buenos Aires (CICPBA) and Agencia Nacional de Ciencia y Tecnologia (ANPCYT) (BID-1728/OC-AR, PAE 22398) to A.M.C. J.M.F. is a fellow of ANPCYT, M.S.M. is a member of the Carrera del Investigador, CONICET, A.M.C. is a member of the Carrera del Investigador, CICPBA, and A.D.M. and M.S.C. are Professors of the UNLP.

References

1. Y. P. Jiao and F. Z. Cui, *Biomed. Mater.* **2**, R24 (2007).
2. L. Santos-Ruiz, D. J. Mowatt, A. Marguerie, D. Tukiainen, M. Kellomäki, P. Törmälä, E. Suokas, H. Arstila, N. Ashammakhi and P. Ferretti, *J. Tissue Eng. Regen. Med.* **1**, 199 (2007).
3. Y. Khan, M. J. Yaszemski, A. G. Mikos and C. T. Laurencin, *J. Bone Joint Surg. Am.* **90**, 36 (2008).
4. E. L. Hedberg, C. K. Shih, J. J. Lemoine, M. D. Timmer, M. A. K. Liebschner, J. A. Jansen and A. G. Mikos, *Biomaterials* **26**, 3215 (2005).
5. P. V. Giannoudis and I. Pountos, *Inyury* **36**, S2 (2005).
6. V. Karageorgiou and D. Kaplan, *Biomaterials* **26**, 5474 (2005).
7. X. Liu and P. X. Ma, *Ann. Biomed. Eng.* **32**, 477 (2004).
8. J. Más Estellés, A. Vidaurre, J. M. Meseguer Dueñas and I. Castilla Cortázar, *J. Mater. Sci. Mater. Med.* **19**, 189 (2008).
9. H. L. Khor, K. W. Ng, A. S. Htay, J. T. Schantz, S. H. Teoh and D. W. Hutmacher, *J. Mater. Sci. Mater. Med.* **14**, 113 (2003).
10. G. C. Eastmond. *Adv. Polym. Sci.* **149**, 59 (1999).
11. M. S. Cortizo, M. S. Molinuevo and A. M. Cortizo, *J. Tissue Eng. Regen. Med.* **2**, 33 (2008).
12. M. S. Cortizo, *J. Appl. Polym. Sci.* **103**, 3785 (2007).
13. M. S. Cortizo, H. A. Andreetta and R. V. Figini, *J. High Res. Chromatogr. Chromatogr. Commun.* **12**, 372 (1989).
14. S. Ghosh, J. C. Viana, R. L. Reis and J. F. Mano, *Acta Biomater.* **4**, 887 (2008).
15. A. D. McCarthy, S. B. Etcheverry, L. Bruzzone and A. M. Cortizo, *Mol. Cell. Biochem.* **170**, 43 (1997).
16. N. C. Partridge, D. Alcorn, V. P. Michelangeli, G. Ryan and T. J. Martin, *Cancer Res.* **43**, 4308 (1983).
17. A. D. McCarthy, T. Uemura, S. B. Etcheverry and A. M. Cortizo, *Int. J. Biochem. Cell Biol.* **36**, 840 (2004).
18. A. M. Cortizo, M. S. Molinuevo, D. A. Barrio and L. Bruzzone, *Int. J. Biochem. Cell Biol.* **38**, 1171 (2006).
19. M. M. Bradford, *Anal. Biochem.* **72**, 248 (1976).
20. A. H. Lebovitz, M. K. Gray, A. C. Chen and J. M. Torkelson, *Polymer* **44**, 2823 (2003).
21. J. S. Oh, A. I. Isayev and M. A. Rogunova, *Polymer* **44**, 2337 (2003).

22. J. Li, S. Guo and X. Li, *Polym. Degrad. Stabil.* **89**, 6 (2005).
23. M. Marx-Figini, *Angew. Makromol. Chem*. **250**, 85 (1997).
24. D. M. Garcia Cruz, J. L. Gomez Ribelles and M. Salmerón Sanchez, *J. Biomed. Mater. Res. B: Appl. Biomater.* **85**, 303 (2008).
25. K. Rezwan, Q. Z. Chen, J. J. Blaker and A. R. Boccacini, *Biomaterials* **27**, 3413 (2006).
26. Y. Koinuma, Y. Murata, T. Otsu, K. Goto, H. Fijiwara and Y. Takita, *Kobunshi Ronbunshu* **54**, 301 (1997).
27. F. Linde and I. Hvid, *J. Biomech.* **22**, 485 (1989).
28. A. Rohlmann, H. Zilch, G. Bergmann and R. Kolbel, *Arch. Orthop. Trauma Surg.* **97**, 95 (1980).
29. M. C. Cortizo, M. F. de Mele and A. M. Cortizo, *Biol. Trace Elem. Res.* **100**, 151 (2004).
30. K. Kawano, S. S. Kantak, M. Murai, C. C. Yao and R. H. Kramer, *Exp. Cell Res.* **262**, 180 (2001).